Effect of Axially Bound Anions on the Electroreduction of Tin(IV) Porphyrins in Tetrahydrofuran†

Karl M. Kadish,* Quan Yun Y. Xu, and G. Bhaskar Maiya
Department of Chemistry, University of Houston, Houston, Texas 77204-5641, U.S.A.
Jean-Michel Barbe and Roger Guilard*
Laboratoire de Synthèse et d'Electrosynthèse Organométallique, Associé au C.N.R.S. (U.A. 33), Faculte des Sciences 'Gabriel', 21100 Dijon, France

The spectroscopic characterization and electrochemistry of $SnL(X)_2$ is presented where L is the dianion of tetra-*p*-tolylporphyrin or tetra-*m*-tolylporphyrin and X is ClO_4^-, Br^-, Cl^-, F^-, or OH^-. In all cases, electroreduction leads to porphyrin π anion radicals and dianions which were characterized in tetrahydrofuran by spectroelectrochemistry and e.s.r. spectroscopy. Dissociation of one ClO_4^- ion from $SnL(ClO_4)_2$ occurs before electroreduction of the complex but no dissociation is observed either before or after electroreduction of $SnL(F)_2$ or $SnL(OH)_2$. In contrast, one Br^- ion dissociates after the first electron addition to $SnL(Br)_2$ while one Cl^- ion dissociates from $SnL(Cl)_2$ after the second electroreduction of this complex.

Numerous chemical,[1] photochemical,[2-12] and electrochemical[13-18] studies involving reduction of tin(IV) metalloporphyrins have appeared in the literature. These complexes can be used as photosensitizers in the reduction of water[5-7,9] and in this regard an initial reduction of the metalloporphyrin is most likely involved. Pulse and steady-state radiolysis experiments showed that the tin(IV) tetraphenylporphyrin π anion radicals generated are short lived in alkaline methanolic solutions and are rapidly converted to chlorins.[15] In contrast, the electrochemical reduction of tin(IV) porphyrins in aqueous solutions leads to chlorins, bacteriochlorins, and porphyrinogens but not to porphyrin π anion radicals as ultimate products in the reaction.[16]

The present work reports a spectroscopic characterization and the detailed electrochemistry and spectroelectrochemistry of $SnL(X)_2$ in tetrahydrofuran (thf) where L is the dianion of tetra-*p*-tolylporphyrin (tptp) or tetra-*m*-tolylporphyrin (tmtp) and X is ClO_4^-, Br^-, Cl^-, F^-, or OH^-. The electrochemical measurements were carried out in water-free thf where protonation of the reduced species does not occur as has been previously reported.[16]

Prior electrochemical studies of $SnL(OH)_2$ (L = tpp, tpc, or tpibc, the dianions of tetraphenylporphyrin, tetraphenylchlorin, and tetraphenylisobacteriochlorin, respectively) show that these complexes can be reduced by one electron in a single step which occurs between $E_{\frac{1}{2}} = -0.89$ and -1.24 V *vs.* saturated calomel electrode (s.c.e.) in thf.[13] The complex $Sn(oep)(OH)_2$ (where oep is the dianion of octaethylporphyrin) undergoes two electroreductions at $E_{\frac{1}{2}} = -0.90$ and -1.30 V in dimethyl sulphoxide (dmso).[18] The products of these electrode reactions were not identified in solution and there is virtually no other electrochemistry of these types of complexes. Thus, this work presents the first systematic study of tin(IV) porphyrins in non-aqueous media as well as the first study which elucidates the effect of different anionic axial ligands on the redox reactions of these complexes.

Experimental

Instrumentation.—I.r. spectra were measured on an IBM FTIR 32 or a Perkin-Elmer PE 580 B spectrometer. Samples were prepared as 1% dispersions in CsI. U.v.–visible spectra were recorded on an IBM model 9430 spectrophotometer. Proton n.m.r. spectra were taken on a General Electric QE-300 spectrometer using tetramethylsilane as the internal reference, with 3 mg of the complex in 1 cm^3 $CDCl_3$ or C_4D_8O. A YSI model 31 conductivity bridge was used to perform conductivity measurements.

Voltammetric measurements were carried out with an EG&G Princeton Applied Research model 174A/175 polarographic analyzer/potentiostat or an IBM EC225 voltammetric analyzer coupled with an EG&G model 9002A X-Y recorder for potential scan rates less than 500 mV s^{-1}. For scan rates ⩾ 500 mV s^{-1} a BAS 100 electrochemical analyzer was used. The working and counter electrodes were a platinum button and a platinum wire, respectively. Potentials were measured *vs.* an s.c.e., which was separated from the bulk solution by a fritted-glass-disc junction.

Unless otherwise noted, 0.1 mol dm^{-3} supporting electrolyte was used for all electrochemical experiments. The sample concentration ranged between 0.5×10^{-4} and 3×10^{-3} mol dm^{-3}. Thin-layer spectroelectrochemical measurements were performed with an EG&G model 173 potentiostat/galvanostat coupled with a Tracor Northern 1710 holographic optical spectrometer multichannel analyzer which gave time-resolved spectral data.[19]

Materials.—Tetrahydrofuran (Aldrich) was purified by distillation prior to use, first from CaH_2, and then from sodium–benzophenone under argon. Tetra-n-butylammonium perchlorate (Alfa) was twice recrystallized from absolute ethanol, dried, and stored under vacuum at 40 °C. Tetra-n-butylammonium bromide (Alfa) was stored in a dry-box and used directly.

The syntheses of $SnL(Cl)_2$ were performed using literature methods.[1] The complexes $SnL(X)_2$ where X = ClO_4^-, Br^-, F^-, and OH^- were obtained by treating $SnL(Cl)_2$ in methylene chloride with the appropriate acid, HX, where X = ClO_4^-, Br^-, or F^- or, for the case of $SnL(OH)_2$, by the reaction of $SnL(Cl)_2$ with a 10% aqueous solution of sodium hydroxide. In all cases hexane was added to the methylene chloride solution. This organic layer was evaporated and the $SnL(X)_2$ complex was crystallized before dryness. Yields were close to 80%.

Results and Discussion

Spectroscopic Characterization of $SnL(X)_2$.—Maximum absorbance wavelengths and molar absorptivities of each

† *Non-S.I. unit employed:* G = 10^{-4} T.

$SnL(X)_2$ complex are presented in Table 1. Each complex belongs to the 'normal' class[20] and has one band [$B(0,0)$] in the Soret region between 420 and 433 nm and two major Q bands between 555 and 609 nm. Table 1 also gives i.r. data for the Sn–X stretch of $SnL(X)_2$. The tin–halide stretching frequencies, ν(Sn–X), vary between 205 and 570 cm^{-1} depending upon the anion, X, and are comparable with the values of 286—634 cm^{-1} for the Ge–X stretch of $Ge(oep)(X)_2$ and $Ge(tpp)(X)_2$ complexes with the same anionic ligands.[21]

As seen in Table 2, the ^1H n.m.r. data of $SnL(X)_2$ are in accord with the i.r. data in that there is the expected downfield shift of the pyrrole protons along the series of anions (δ for OH^- < δ for ClO_4^-). This shift is due to the increased electron density on the macrocycle upon going from a ClO_4^- to an OH^- counter ion.[21] No significant changes in the methyl proton signals are detected (2.73—2.74 for tptp and 2.65—2.69 for tmtp).

The conductivities of 1×10^{-3} mol dm^{-3} solutions of $Sn(tptp)(X)_2$ in thf are as follows: 3.9 for $X = ClO_4^-$, 0.2 for $X = Br^-$, and 0.2 Ω^{-1} cm^2 mol^{-1} for $X = F^-$. A millimolar solution of $NBu^n_4ClO_4$ has a conductivity of 5.0 Ω^{-1} cm^2 mol^{-1} in thf. Thus, on the basis of the data, it can be concluded that $SnL(Br)_2$ and $SnL(F)_2$ are virtually undissociated in the thf while $SnL(ClO_4)_2$ (L = tptp) undergoes an ionic dissociation and binding of thf as shown in equation (1).

$$Sn(tptp)(ClO_4)_2 + thf \rightleftharpoons [Sn(tptp)(ClO_4)(thf)]^+ + ClO_4^- \quad (1)$$

An anisotropy of the porphyrin macrocycle would occur if two different axial ligands were bound to the tin(IV) ion in *trans* positions[22] as would be the case for $[Sn(tptp)(ClO_4)(thf)]^+$. This assignment is supported by the ^1H n.m.r. data for $SnL(ClO_4)_2$ and $SnL(Br)_2$ (L = tptp) in C_4D_8O as shown in Figure 1. The two well resolved doublets of $Sn(tptp)(Br)_2$ at 7.62 and 8.19 are due to the coupling of the *ortho* and *meta* protons on the phenyl group. The perchlorate salt has multiplets at 7.63 and 8.18. Integration of the peak area in Figure 1(*a*) gives an 8:8:8 ratio for the β-pyrrole:*ortho*:*meta* protons. The small peak at 9.50 in Figure 1(*b*) may be due to the pyrrole proton resonance of residual undissociated $Sn(tptp)(ClO_4)_2$. The integrated area under this peak is approximately 10% of the area of the pyrrole proton resonances of $[Sn(tptp)(ClO_4)(thf)]^+$

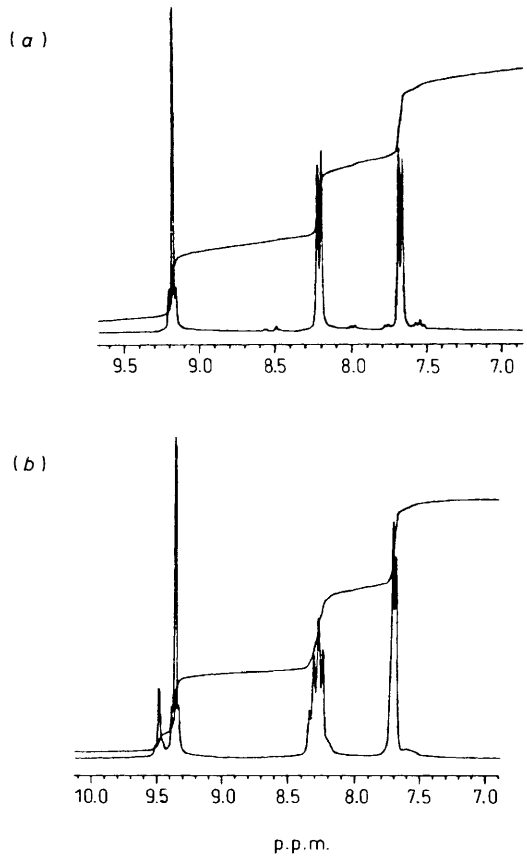

Figure 1. Proton n.m.r. spectra of (*a*) $Sn(tptp)(Br)_2$ and (*b*) $Sn(tptp)(ClO_4)_2$ recorded at 300 MHz in C_4D_8O

Table 1. I.r.[a] and u.v.–visible[b] spectral data for $SnL(X)_2$

Porphyrin, L	Anion, X	ν(Sn–X)/ cm^{-1}	λ/nm (10^{-4} ε/dm^3 mol^{-1} cm^{-1})		
			B(0,0)	*Q*(1,0)	*Q*(0,0)
tptp	OH^-	560	427 (49.1)	563 (2.0)	602 (1.4)
	F^-	550	423 (64.4)	557 (2.3)	597 (2.1)
	Cl^-	309	428 (46.6)	562 (1.8)	603 (1.4)
	Br^-	205	433 (77.6)	568 (2.8)	609 (3.0)
	ClO_4^-	225	425 (52.1)	557 (2.2)	598 (1.5)
tmtp	OH^-	570	426 (51.7)	561 (2.2)	601 (1.3)
	F^-	550	420 (64.4)	555 (2.5)	594 (1.3)
	Cl^-	303	428 (63.4)	564 (1.9)	603 (1.4)
	Br^-	205	432 (74.8)	569 (2.9)	608 (2.6)
	ClO_4^-	225	423 (52.5)	555 (2.2)	595 (1.0)

[a] CsI pellets. [b] Solvent = thf.

Table 2. Proton chemical shifts and ^1H–$^{117,119}Sn$ coupling constants of $SnL(X)_2$ in $CDCl_3$

		Pyrrole H		Phenyl H (*ortho*)		Phenyl H (*meta*)		Phenyl H (*para*)		*p*-CH_3		*m*-CH_3		Sn–OH	
L	X	*m i*	δ	*m i*	δ	*m i*	δ	*m i*	δ	*m i*	δ	*m i*	δ	*m i*	δ
tptp	OH^-	s 8	9.13 (12.24)	d 8	8.21	d 8	7.62			s 12	2.73			s 2	−7.49
	F^-	s 8	9.21 (14.44)	d 8	8.21	d 8	7.62			s 12	2.73				(36.08)
	Cl^-	s 8	9.21 (15.25)	d 8	8.19	d 8	7.61			s 12	2.73				
	Br^-	s 8	9.20 (14.93)	d 8	8.19	d 8	7.62			s 12	2.73				
	ClO_4^-	s 8	9.30 (17.41)	m 8	8.18	m 8	7.63			s 12	2.74				
tmtp	OH^-	s 8	9.17 (14.37)	m 8	8.14			m 8	7.65			s 12	2.69	s 2	−6.9
	F^-	s 8	9.22 (12.81)	m 8	8.15			m 8	7.67			s 12	2.68		
	Cl^-	s 8	9.21 (15.32)	m 8	8.13			m 8	7.69			s 12	2.66		
	Br^-	s 8	9.20 (15.18)	m 8	8.11			m 8	7.67			s 12	2.65		
	ClO_4^-	s 8	9.30 (17.39)	m 8	8.09			m 8	7.68			s 12	2.67		

Coupling constants (Hz) in parentheses. *m* = Number of lines, *i* = number of protons; s = singlet, d = doublet, and m = multiplet.

Table 3. Half-wave potentials (*V vs.* s.c.e.) for reduction of $SnL(X)_2$ in thf, 0.1 mol dm^{-3} $NBu^n_4ClO_4$

		Reduction		
L	X	1st	2nd	$\Delta E_{\frac{1}{2}}$
tptp	OH^-	−0.86	−1.32	0.46
	F^-	−0.77	−1.23	0.46
	Cl^-	−0.78	−1.16[a]	*b*
	Br^-	−0.79[a]	−1.00	*b*
	ClO_4^-	−0.48	−0.99	0.51
tmtp	OH^-	−0.85	−1.29	0.44
	F^-	−0.75	−1.23	0.48
	Br^-	−0.76[a]	−0.97	*b*
	ClO_4^-	−0.47	−0.97	0.50

[a] E_{pc} measured at 0.1 V s^{-1}. [b] $\Delta E_{\frac{1}{2}}$ could not be calculated because one of the two electrode reactions is irreversible.

and this indicates that 90% of $Sn(tptp)(ClO_4)_2$ is converted into $[Sn(tptp)(ClO_4)(thf)]^+$ in thf. A similar observation can be made in the case of $Sn(tmtp)(ClO_4)_2$.

A dissociation of ClO_4^- as shown in equation (1) is also supported by the long-range coupling (over four bonds) of the tin nucleus and the β-pyrrole protons of $Sn(tptp)(ClO_4)_2$ in C_4D_8O. As seen in Figure 1, there are satellite peaks flanking the β-pyrrole proton resonance for both $SnL(Br)_2$ and $SnL(ClO_4)_2$ (L = tptp) which can be assigned to long-range coupling to the tin nucleus over four bonds.[23] Similar observations are made for each of the complexes reported in this study and the ^1H–$^{117,119}Sn$ coupling constants are given in Table 2 which lists the ^1H n.m.r. data for each of the ten complexes investigated.

The ^1H–$^{117,119}Sn$ coupling constants range between 12.24 Hz for $Sn(tptp)(OH)_2$ and 17.41 Hz for $Sn(tptp)(ClO_4)_2$. It is interesting that $SnL(Cl)_2$ has a larger coupling constant than its bromide, hydroxide, and fluoride analogues. The coupling constant of $Sn(tpp)(Cl)_2$ is also larger than that of $Sn(tpp)(OH)_2$ and this has been ascribed to differences in the p_π–d_π back bonding abilities of Cl^- and OH^- with the tin nucleus.[23] This will augment the σ overlap between tin and the pyrrolic nitrogen atoms, increasing the Fermi contact and, implicitly, the transmission of spin–spin coupling to the β-pyrrole proton.[24] A similar mechanism may be operative in the case of positively charged $[SnL(ClO_4)(thf)]^+$ complexes compared to other undissociated tin(IV) porphyrins of the form $SnL(X)_2$ and this can explain the higher magnitudes of the coupling constants observed for the former complexes.

Electroreduction of $SnL(F)_2$ *and* $SnL(OH)_2$.—The electroreduction of $SnL(F)_2$ and $SnL(OH)_2$ is uncomplicated and proceeds *via* two reversible one-electron additions in thf. Dissociation of the anionic F^- or OH^- ligand does not occur on the cyclic voltammetric time-scale and similar reductive behaviour occurs for each of the tptp and tmtp complexes whose potentials are listed in Table 3. The behaviour of $SnL(OH)_2$ (L = tptp or tmtp) is similar to that of $Sn(oep)(OH)_2$[18] in that there are no coupled chemical reactions on the time-scale of the electroreductions. As will be shown later, both electrode reactions occur at the porphyrin π-ring system. The absolute potential differences between the two reductions of $SnL(F)_2$ and $SnL(OH)_2$ vary between 0.44 and 0.48 V depending upon the specific porphyrin ring and axial ligand and are within the range of values generally observed for ring-centred reductions of metalloporphyrin complexes.[25]

Electroreduction of $SnL(ClO_4)_2$.—A cyclic voltammogram of

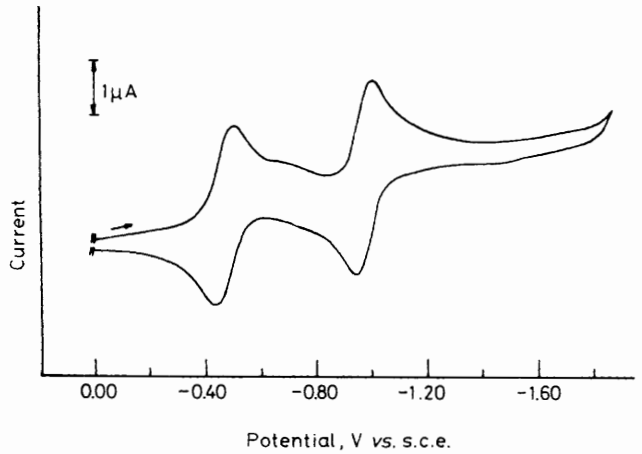

Figure 2. Cyclic voltammogram of $Sn(tmtp)(ClO_4)_2$ in thf, 0.1 mol dm^{-3} $NBu^n_4ClO_4$. Scan rate = 0.1 V s^{-1}

$Sn(tmtp)(ClO_4)_2$ in thf is shown in Figure 2. The cyclic voltammograms of $SnL(ClO_4)_2$ (L = tmtp or tptp) are similar to each other in thf and are also similar to the voltammograms of $SnL(F)_2$ and $SnL(OH)_2$ in that there are no coupled chemical reactions on the time-scale of cyclic voltammetry. The neutral $SnL(ClO_4)_2$ complexes are dissociated in thf (see n.m.r. and conductivity data) and thus the electrochemistry actually refers to $[SnL(ClO_4)(thf)]^+$.

As seen in Figure 2, $[Sn(tmtp)(ClO_4)(thf)]^+$ undergoes two reversible one-electron reductions located at $E_{\frac{1}{2}} = -0.47$ and −0.97 V. There is also a small peak at $E_p = -0.72$ V. This peak is assigned to the reduction of undissociated $Sn(tmtp)(ClO_4)_2$ which should occur at more negative potentials than positively charged $[Sn(tmtp)(ClO_4)(thf)]^+$. The small current at $E_p = -0.72$ V suggests that $Sn(tmtp)(ClO_4)_2$ is mainly dissociated in thf, a conclusion which is also supported by the ^1H n.m.r. spectrum and conductivity data for this complex.

The potential separations between $E_{\frac{1}{2}}$ for the two main reductions of $Sn(tmtp)(ClO_4)_2$ and $Sn(tptp)(ClO_4)_2$ are 0.50 and 0.51 V indicating ring-centred reactions.[25] The values of $i_p/v^{\frac{1}{2}}$ are constant, thus suggesting diffusion-controlled reductions.[26] This reversibility contrasts with the irreversible reductions which have been reported for other tin(IV) porphyrins in aqueous solutions.[16]

An example of the spectral changes recorded during controlled-potential electroreduction of $Sn(tptp)(ClO_4)_2$ in thf is shown in Figure 3. The presence of isosbestic points at 434, 578, and 612 nm indicates an equilibrium between the initial dissociated $[Sn(tptp)(ClO_4)(thf)]^+$ complex and the singly reduced species. The final spectrum after controlled-potential electroreduction has bands at 717 and 764 nm, and is characteristic of a porphyrin π anion radical.[25,27] This reduction is reversible on the thin-layer spectroelectrochemical time-scale (1—5 min) and the spectrum of the starting species could be regenerated upon controlled-potential reoxidation at −0.30 V.

Exhaustive electrolysis of $Sn(tptp)(ClO_4)_2$ at −0.70 V gives a solution whose e.s.r. spectrum is also consistent with formation of a porphyrin π anion radical. The values of $g_\perp$ and $g_\parallel$ are 2.002 and 1.987, respectively, and reflect the pseudo-axial symmetry of the reduced species.[28] The peak-to-peak separation, ΔH_{pp}, for reduced $SnL(ClO_4)_2$ is 10.5 G for L = tptp and 10.1 G for L = tmtp.

The addition of two electrons to $Sn(tptp)(ClO_4)_2$ generates a species which has bands at 422 and 572 nm and no absorbances between 600 and 800 nm. Complexes of $Sn(tpc)(Cl)_2$ and $Sn(tpibc)(Cl)_2$ in benzene exhibit sharp bands at 630 and 612 nm, respectively.[6] The lack of these bands after electroreduction

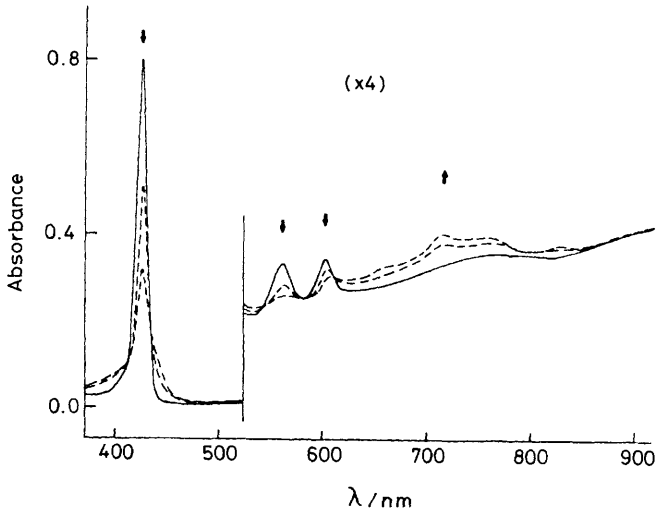

Figure 3. Time-resolved electronic absorption spectra obtained during controlled-potential reduction of $Sn(tptp)(ClO_4)_2$ in thf, 0.2 mol dm^{-3} $NBu^n_4ClO_4$ at −0.70 V

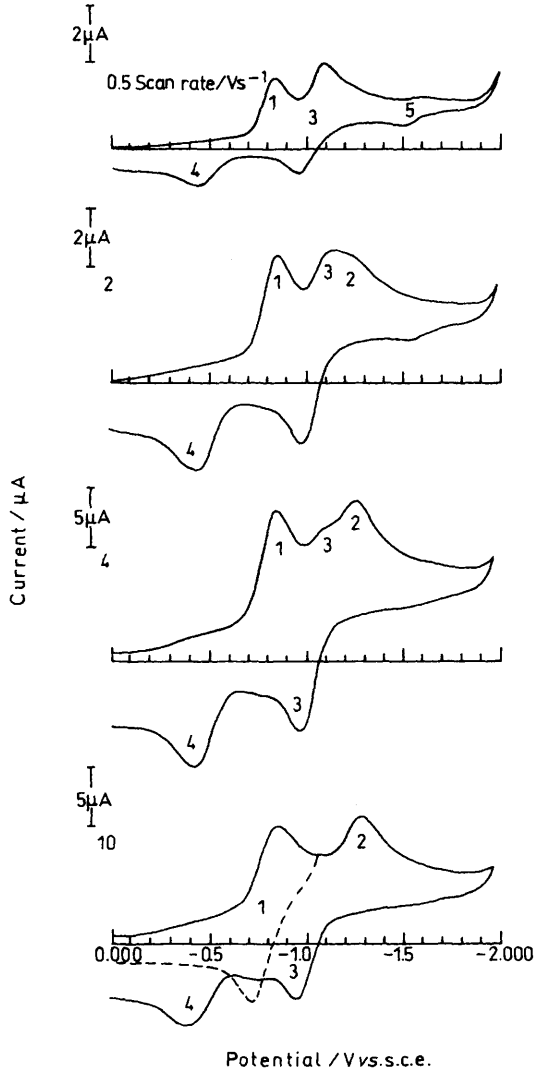

Figure 4. Cyclic voltammograms of $Sn(tptp)(Br)_2$ in thf, 0.1 mol dm^{-3} $NBu^n_4ClO_4$ at scan rates of 0.5, 2, 4, and 10 V s^{-1}

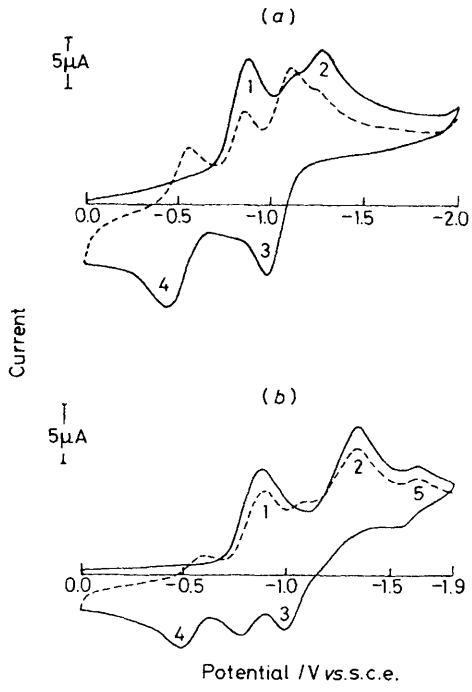

Figure 5. Multiscan cyclic voltammograms of (*a*) $Sn(tptp)(Br)_2$ and (*b*) $Sn(tptp)(Cl)_2$ in thf, 0.1 mol dm^{-3} $NBu^n_4ClO_4$. (——) First scan; ( ) second scan. Scan rate = 4 V s^{-1}

of $Sn(tptp)(ClO_4)_2$ in thf suggests the absence of a neutral chlorin or a neutral isobacteriochlorin as an ultimate product of the overall two-electron electroreduction.

Electroreduction of $SnL(Br)_2$.—The electroreduction of $SnL(Br)_2$ differs from that of $SnL(OH)_2$, $SnL(F)_2$, and $SnL(ClO_4)_2$ in that the number and positions of the observed reduction peaks depend upon both the scan number and the potential scan rate. This is illustrated by the data in Figure 4 which shows cyclic voltammograms for the reduction of $Sn(tptp)(Br)_2$ at scan rates between 0.5 and 10 V s^{-1}. A similar voltammetric behaviour is observed for $Sn(tmtp)(Br)_2$.

At 0.5 V s^{-1} $Sn(tptp)(Br)_2$ undergoes one irreversible reduction (process 1), one irreversible reoxidation (process 4), and one reversible reduction–oxidation couple (process 3). There is also a reversible process (5) with reduced intensity at a more negative potential. As the scan rate is increased from 0.5 to 10 V s^{-1} the cathodic currents for processes 3 and 5 decrease while a new cathodic peak (process 2) appears. At 10 V s^{-1} only peaks 1—4 remain, but none of these is directly coupled to each other. This is demonstrated by the fact that peak 4 disappears and process 1 becomes almost totally reversible at 10 V s^{-1} when the scan direction is reversed at potentials before the second reduction peak. This is shown by the dashed line in Figure 4. A well defined reversible reduction (process 1) is also observed for $Sn(tptp)(Br)_2$ when the thf solution contains a mixture of 0.1 mol dm^{-3} $NBu^n_4ClO_4$ and 1 mol dm^{-3} NBu^n_4Br.

A multiscan cyclic voltammogram of $Sn(tptp)(Br)_2$ is shown in Figure 5(*a*). There are two irreversible cathodic peaks (processes 1 and 2) on the first reductive scan, but on the second reductive scan (dashed line) the currents for peaks 1 and 2 decrease while those for new cathodic peaks 3 and 4 increase. Under these conditions reversible reactions can be seen at $E_{\frac{1}{2}} = -0.51$ and -1.04 V for processes 3 and 4. The separation between these $E_{\frac{1}{2}}$ values on the second scan is 0.53 V, suggesting that these two reductions occur at the porphyrin π-ring system.[25]

Table 4. Maximum absorbance wavelengths ($\lambda_{max.}$) and molar absorption coefficients (ε) of neutral, singly reduced, and doubly reduced $SnL(X)_2$ complexes in thf, 0.2 mol dm^{-3} $NBu^n_4ClO_4$

Reaction	L	X	$\lambda_{max.}$/nm (10^{-4} ε/dm^3 mol^{-1} cm^{-1})		
None	tptp	OH^-	427 (49.1)	563 (2.0)	602 (1.4)
		F^-	423 (64.4)	557 (2.3)	597 (2.1)
		Cl^-	428 (46.6)	562 (1.8)	603 (1.4)
		Br^-	433 (77.6)	568 (2.8)	608 (3.0)
		ClO_4^-	428 (52.1)	563 (2.2)	603 (1.5)
	tmtp	OH^-	424 (39.6)	560 (0.8)	601 (0.6)
		F^-	421 (64.4)	555 (2.5)	594 (1.3)
		Br^-	433 (74.8)	567 (2.9)	607 (2.6)
		ClO_4^-	428 (52.5)	563 (2.2)	603 (1.0)
One-electron reduction *	tptp	OH^-	420 (12.2) 452 (14.7)	745 (1.2)	883 (0.6)
		F^-	444 (23.9)	725 (2.9)	859 (1.5)
		Cl^-	418 (10.0) 448 (7.3)		743 (0.9)
		Br^-	436 (17.4)	716 (2.3)	755 (2.2)
		ClO_4^-	428 (18.1)	717 (2.9)	764 (1.0)
	tmtp	OH^-	424 (13.8)		722 (0.4)
		F^-	424 (14.6) 442 (15.2)	719 (1.8)	857 (1.0)
		Br^-	428 (14.3) 452 (14.1)		741 (2.4)
		ClO_4^-	427 (23.2)	719 (1.9)	831 (0.8)
Two-electron reduction *	tptp	OH^-	450 (22.7)	604 (3.1)	
		F^-	438 (21.1)	595 (2.9)	
		Cl^-	423 (7.8)	572 (0.6)	
		Br^-	423 (14.6)	570 (2.6)	
		ClO_4^-	422 (6.8)	572 (1.6)	
	tmtp	OH^-	423 (8.9)	570 (0.9)	
		F^-	437 (12.2)	595 (2.1)	
		ClO_4^-	427 (7.9)	572 (1.9)	

* By controlled-potential electrolysis.

Table 5. E.s.r. data for singly reduced $SnL(X)_2$ in thf, 0.2 mol dm^{-3} $NBu^n_4ClO_4$ at 115 K

L	X	$g_\perp$	$g_\parallel$	ΔH_{pp}/G
tptp	F^-	2.004	1.988	8.6
	Cl^-	2.004		6.9
	Br^-	2.003		9.3
	ClO_4^-	2.002	1.987	10.5
tmtp	F^-	2.002	1.989	12.6
	Br^-	2.003		10.9
	ClO_4^-	2.003		10.1

Electroreduction of $Sn(tptp)(Cl)_2$.—A cyclic voltammogram illustrating the reduction of $Sn(tptp)(Cl)_2$ in thf is shown in Figure 5(*b*). Only two reductions (processes 1 and 2) are observed on the first scan, but two additional quasi-reversible reductions (processes 3 and 4) are observed on the second cathodic scan (dashed line). Process 1 is different from that of $Sn(tptp)(Br)_2$ in that it is quasi-reversible and becomes almost reversible when the potential scan is reversed before the second reduction peak. However, process 2 is similar to that of $Sn(tptp)(Br)_2$ in that the reduction is irreversible and a chemical reaction follows this electron-transfer step. Reoxidation peaks 3 and 4 are observed at $E_p = -0.51$ and -0.97 V and are not directly coupled to the two initial reduction peaks 1 and 2. There is also a reversible process with reduced currents at around $E_{\frac{1}{2}} = -1.5$ V. The origin of this peak is unknown.

The formation of first a porphyrin π anion radical and then a dianion upon electroreduction of $Sn(tptp)(Cl)_2$ in thf was ascertained by monitoring the thin-layer spectra. The resulting spectral data are summarized in Table 4. In each case the singly reduced complex has broad bands between 700 and 900 nm which are characteristic of a porphyrin π anion radical. The singly reduced $Sn(tptp)(Cl)_2$ is e.s.r. active after controlled-potential electrolysis at -0.90 V. The e.s.r. data are given in Table 5 which also lists values for the other singly reduced complexes of $SnL(X)_2$.

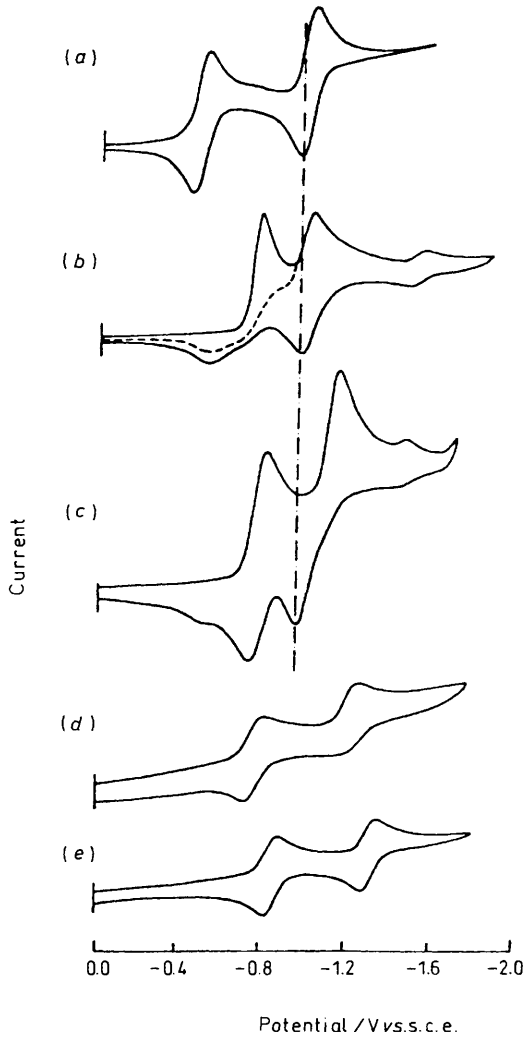

Figure 6. Cyclic voltammograms of $Sn(tptp)(X)_2$ in thf, 0.1 mol dm^{-3} $NBu^n_4ClO_4$. Scan rate = 0.1 V s^{-1}. X = ClO_4 (*a*), Br (*b*), Cl (*c*), F (*d*), or OH (*e*)

Mechanism for Electroreduction of $SnL(X)_2$.—There are two possible pathways for reduction of each $SnL(X)_2$ complex. These involve the reduction of neutral and singly reduced tin(IV) porphyrins containing either one or two axially bound anionic ligands. The neutral compounds which are totally associated in thf are $SnL(F)_2$ and $SnL(OH)_2$ and these undergo two well defined reductions. Reversible well defined processes are also obtained for $SnL(ClO_4)_2$. This latter compound is dissociated in thf and exists as $[SnL(ClO_4)(thf)]^+$ in solution as shown by the n.m.r. data. On the other hand, a dissociation of the anionic ligands from $SnL(Br)_2$ or $SnL(Cl)_2$ may or may not occur after electroreduction depending upon the potential scan rate and the overall scan range. In these cases the voltammograms are more complicated and give reduction and oxidation peaks which vary with scan rate as shown in Figures 4 and 5.

On the basis of the voltammetric and spectroscopic data, the

Table 6. Half-wave potential (V *vs.* s.c.e.)[a] for reduction of $[SnLX(thf)]^+$ in thf, 0.1 mol dm^{-3} $NBu^n_4ClO_4$

Compound	$E_{\frac{1}{2}}(1)$	$E_{\frac{1}{2}}(2)$	$\Delta E_{\frac{1}{2}}$
$[Sn(tptp)Cl(thf)]^+$	−0.54	−1.05	0.51
$[Sn(tptp)Br(thf)]^+$	−0.51	−1.04	0.53
$[Sn(tptp)(ClO_4)(thf)]^{+b}$	−0.48	−0.99	0.51
$[Sn(tmtp)Br(thf)]^+$	−0.48	−1.02	0.54
$[Sn(tmtp)(ClO_4)(thf)]^{+b}$	−0.47	−0.97	0.50

[a] Measured at 4 V s^{-1}. [b] Measured at 0.1 V s^{-1}.

mechanism shown in the Scheme can be proposed for the overall electroreduction of each $SnL(X)_2$ complex in thf. A thf molecule is shown as co-ordinated to $[SnLX(thf)]^+$ where X = Cl^-, Br^-, or ClO_4^- but may or may not remain bound after electroreduction. The direct formation of $[SnLX(thf)]^+$ from $SnL(X)_2$ only occurs for X = ClO_4^-. In the case of X = Cl^- or Br^- the mixed-ligand complex is generated by electro-oxidation of SnLX as shown in Figure 5.

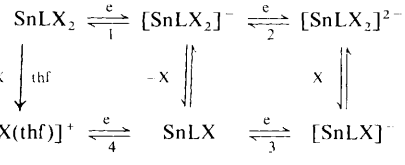

Scheme.

The above mechanism is best illustrated by comparing voltammograms for the five $Sn(tptp)(X)_2$ compounds at a scan rate of 0.1 V s^{-1} (Figure 6). Under these conditions, $SnL(OH)_2$ and $SnL(F)_2$ (L = tptp) are reversibly reduced according to processes 1 and 2 in the Scheme. The salt $Sn(tptp)(ClO_4)_2$ dissociates to give $[Sn(tptp)(ClO_4)(thf)]^+$ and this positively charged species is reversibly reduced by processes 4 and 3 in the Scheme. One halide ion dissociates from singly and/or doubly reduced $SnL(Br)_2$ and $SnL(Cl)_2$ (L = tptp) and, in these cases, the reduction–oxidation reactions proceed through processes 1—4. This effect of the axial anionic ligand on the electroreduction of $SnL(X)_2$ in thf is consistent with the increasing order in binding ability of the anion X^- to the porphyrin metal centre which for the case of FeL(X) or MnL(X) is as follows:[29] $OH^- > F^- > Cl^- > Br^- > ClO_4^-$.

A similar 'box mechanism' to that in the Scheme has been demonstrated to exist for M(tpp)(X) complexes where M = Fe^{III},[29,30] Cr^{III},[31,32] and $Mo^{V}O$.[33,34] However, in the above examples, the electroreduction occurs at the porphyrin metal centre while in the case of $SnL(X)_2$, the electroreduction clearly occurs at the porphyrin π-ring system.

The second potential scan in the reduction of $SnL(X)_2$ will result in the formation of $[SnL(X)(thf)]^+$ where X = Cl^-, Br^-, or ClO_4^-. The specific potentials for reduction of these dissociated positively charged complexes are listed in Table 6. The effect of anions on $E_{\frac{1}{2}}$ for each reduction of $[SnL(X)(thf)]^+$ parallels the effect for $SnL(X)_2$ and follows the order $Cl^- > Br^- > ClO_4^-$. The absolute potential differences ($\Delta E_{\frac{1}{2}}$) between the two reactions of $SnL(X)_2$ and $[SnLX(thf)]^+$ are comparable but the latter series of complexes are more easily reduced as expected for a positively charged species. For example, the difference in $E_{\frac{1}{2}}$ between the reduction of $Sn(tptp)(Cl)_2$ and $[Sn(tptp)Cl(thf)]^+$ amounts to 240 mV.

Finally, the controlled-potential one-electron reduction of $Sn(tptp)(X)_2$ generates a stable π anion radical in dry thf. However, the addition of water to solutions of these π anion radicals leads to absorption spectra which are similar to those of the initial porphyrin. The spectra also have a peak at *ca.* 620 nm which is typical of a tin(IV) chlorin[6] and this suggests that protonation and disproportionation of the π-anion radical occurs to generate a mixture of the initial tin(IV) porphyrin and a tin(IV) chlorin. This reaction occurs for all of the $SnL(X)_2$ derivatives except for $SnL(F)_2$ and $SnL(OH)_2$.

Acknowledgements

The support of the National Science Foundation (Grants No. CHE-8515411 and No. INT-8412696) and the Centre National de la Recherche Scientifique is gratefully acknowledged.

References

1 A. H. Corwin and O. D. Collins III, *J. Org. Chem.*, 1962, **27**, 3060.
2 D. G. Whitten, *Acc. Chem. Res.*, 1980, **13**, 83.
3 W. Kruger and J-H. Fuhrhop, *Angew. Chem., Int. Ed. Engl.*, 1981, **21**, 131.
4 J-H. Fuhrhop, W. Kruger, and H. H. David, *Liebigs Ann. Chem.*, 1983, 204.
5 W. Szulbinski and J. W. Strojek, *Inorg. Chim. Acta*, 1986, **118**, 91.
6 Y. Harel and J. Manassen, *J. Am. Chem. Soc.*, 1977, **99**, 5817.
7 K. Chandrasekaran, C. Giannotti, K. Monserrat, J. P. Otruba, and D. G. Whitten, *J. Am. Chem. Soc.*, 1982, **104**, 6200.
8 H. Inoue, K. Chandrasekaran, and D. G. Whitten, *J. Photochem.*, 1985, **30**, 269.
9 D. G. Whitten, J. C. Yau, and F. A. Carroll, *J. Am. Chem. Soc.*, 1971, **93**, 2291.
10 E. Breslow, R. Chandra, and A. Kappas, *J. Biol. Chem.*, 1986, **261**, 3135.
11 P. Sayer, M. Gouterman, and C. R. Connell, *Acc. Chem. Res.*, 1982, **15**, 73.
12 S. Baral, P. Hambright, and P. Neta, *J. Phys. Chem.*, 1984, **88**, 1595.
13 C. Cloutour, C. Debaig-Valade, and J-C. Pommier, *J. Organomet. Chem.*, 1981, **220**, 21.
14 R. H. Felton and H. Linschitz, *J. Am. Chem. Soc.*, 1966, **88**, 1113.
15 J-H. Fuhrhop and T. Lumbantobing, *Tetrahedron Lett.*, 1970, 2315.
16 W. Szulbinski, J. Zak, and J. W. Strojek, *J. Electroanal. Chem.*, 1987, **226**, 159.
17 K. M. Kadish, C. Swistak, B. Boisselier-Cocolios, J-M. Barbe, and R. Guilard, *Inorg. Chem.*, 1986, **25**, 4336.
18 J-H. Fuhrhop, K. M. Kadish, and D. G. Davis, *J. Am. Chem. Soc.*, 1973, **95**, 5140.
19 X-Q. Lin and K. M. Kadish, *Anal. Chem.*, 1985, **57**, 1498.
20 M. Gouterman, in 'The Porphyrins,' ed. D. Dolphin, Academic Press, New York, 1978, vol. 3, ch. 1 and refs therein.
21 K. M. Kadish, Q. Y. Xu, J-M. Barbe, J. E. Anderson, E. Wang, and R. Guilard, *Inorg. Chem.*, 1987, **27**, 691.
22 C. A. Busby and D. Dolphin, *J. Magn. Reson.*, 1976, **23**, 211.
23 L. R. Milgrom and R. N. Sheppard, *J. Chem. Soc., Chem. Commun.*, 1985, 350.
24 R. J. Abraham, G. E. Hawkes, and K. M. Smith, *J. Chem. Soc., Perkin Trans. 2*, 1974, 627.
25 K. M. Kadish, *Prog. Inorg. Chem.*, 1986, **34**, 435.
26 R. S. Nicholson and I. Shain, *Anal. Chem.*, 1966, **36**, 704.
27 R. H. Felton, in 'The Porphyrins,' ed. D. Dolphin, Academic Press, New York, 1978, vol. 5, ch. 3.
28 J. Fajer and M. S. Davis, in 'The Porphyrins,' ed. D. Dolphin, Academic Press, New York, 1979, vol. 4, ch. 4.
29 K. M. Kadish, in 'Iron Porphyrins,' Part 2, eds. A. B. P. Lever and H. B. Gray, Addison Wesley, Reading, Massachusetts, 1983, pp. 161—249.
30 L. A. Bottomley and K. M. Kadish *Inorg. Chem.*, 1981, **20**, 1348.
31 L. A. Bottomley and K. M. Kadish, *Inorg. Chem.*, 1983, **22**, 342.
32 L. A. Bottomley and K. M. Kadish, *J. Chem. Soc., Chem. Commun.*, 1981, 1212.
33 K. M. Kadish, T. Malinski, and H. Ledon, *Inorg. Chem.*, 1982, **21**, 2982.
34 Y. Matsuda, S. Yamada, and Y. Murakami, *Inorg. Chem.*, 1981, **20**, 2239.

Received 19*th August* 1988; *Paper* 8/03363C